

SGORP: A Subgradient-based Method for d -Dimensional Rectilinear Partitioning

MUHAMMED FATİH BALIN, XIAOJING AN, ABDURRAHMAN YAŞAR, and ÜMIT V. ÇATALYÜREK*, School of Computational Science and Engineering, Georgia Institute of Technology, USA

Partitioning for load balancing is a crucial first step to parallelize any type of computation. In this work, we propose SGORP, a new spatial partitioning method based on *Subgradient Optimization*, to solve the d -dimensional Rectilinear Partitioning Problem (RPP). Our proposed method allows the use of customizable objective functions as well as some user-specific constraints, such as symmetric partitioning on selected dimensions. Extensive experimental evaluation using over 600 test matrices shows that our algorithm achieves favorable performance against the state-of-the-art RPP and Symmetric RPP algorithms. Additionally, we show the effectiveness of our algorithm to do application-specific load balancing using two applications as motivation: Triangle Counting and Sparse Matrix Multiplication (SpGEMM), where we model their load-balancing problems as 3-dimensional RPPs.

CCS Concepts: • **Computing methodologies** → **Shared memory algorithms**.

Additional Key Words and Phrases: Spatial partitioning, rectilinear partitioning, symmetric partitioning.

1 INTRODUCTION

Parallel computing systems have become ubiquitous, and ever-increasing data necessitates their use. Mapping the data and the computation onto the processors of these parallel systems is usually the initial parallelization step. However, a significant amount of those data are irregular, i.e., they do not have easily observable patterns among their elements. Therefore, efficient partitioning of the data and computation for mapping is a difficult problem. In some applications, computational dependency and data can be represented as graphs/hypergraphs by defining interactions among entities. Connectivity-based methods [3, 6, 15, 18] can be used to partition those type of irregular data. Another large class of irregular data comes from applications that deals with entities in multi-dimensional spaces, such as 3D space and time [14]. In many cases, like n -body problems [17, 30, 37], computational dependencies depends on spatial relations of the entities, hence it would be preferred to partition the data (and work) by keeping the entities that are close-by in space together. Spatial partitioning achieves that by taking the d -dimensional spatial coordinates of the input and dividing the space into multi-dimensional rectangles and minimizing the maximum load (hence minimizing the load imbalance) [2, 24, 29, 33, 35]. In this work, we tackle the generalized spatial partitioning problem of irregular data for parallel processing.

Many different spatial partitioning strategies have been proposed based on various structural constraints, balancing between flexibility and communication patterns [2, 13, 24, 33, 35]. Among these methods, rectilinear partitioning (a.k.a., generalized block distribution) [13, 24] partitions two-dimensional space using straight lines parallel to each dimension. It is one of the most widely used techniques due to its simplicity and resulting well-structured communication pattern.

The regularity of the partitioned space makes rectilinear partitioning ideal for many applications. Limiting the number of neighbors restricts communication into logical rows or columns of virtual mesh topologies and is beneficial for communication patterns, simplifying the communication and

*Also with Amazon Web Services. This publication describes work performed at the Georgia Institute of Technology and is not associated with Amazon.

reasoning of many computational kernels. For instance, matrix/tensor kernels, such as multiplication, can be naturally represented using rectilinear partitioning. These properties make rectilinear partitioning a more attractive choice than other types of spatial partitioning techniques.

The optimal one-dimensional Rectilinear Partitioning Problem (RPP) has a polynomial-time algorithm [28]. However, multidimensional RPP is NP-hard [13]. Very recently, [38] shows that the symmetric variant of RPP is also NP-hard. However, in the multidimensional case, the conditional RPP, which finds the optimal partitioning when partitions of all but one dimension are fixed, is polynomial-time solvable [28].

In this paper, we propose SGORP, a Subgradient Optimization [4] based method to tackle the more general, multi-dimensional RPP. A multi-dimensional rectilinear partition of a given d -dimensional domain arises when each of the parts are rectangular volumes whose dimensions exactly match that of each neighbor at each face. Finding a rectilinear partitioning of a given d -dimensional domain is useful not only in applications where the data is already in a d -dimensional space but also in applications where the computation can be represented in a d -dimensional space. Consider Matrix Multiplication as an example. Here, the input data lies in a 2-dimensional space yet the computation is best represented in a 3-dimensional space. Thus, there is a need for methods tackling the RPP in higher dimensions.

We demonstrate our method is efficient in finding high-quality solutions for multiple variants of rectilinear partitioning. One important property of our proposed method is that it allows the use of customizable objective functions, such as minimizing the sum of loads of combinations of tiles with arbitrary partition sizes for each dimension.

The main contributions of this work are:

- Presenting a formulation for the Rectilinear Partitioning Problem (RPP) for the continuous domain (Section 3),
- Proposing and implementing an efficient iterative method for the RPP that generalizes to an arbitrary d dimensions and can also solve the Symmetric RPP (SRPP) via constraints (Section 4),
- Demonstrating the superiority of the proposed method over the existing state-of-the-art, applying an extensive experimental evaluation on more than 600 real-world matrices (Section 6.2),
- Demonstrating the effectiveness of different customizations of SGORP in 2-dimensional (RPP and SRPP), and 3-dimensional (Triangle Counting and Generalized Sparse Matrix-Matrix Multiplication (SpGEMM)) use-cases (Section 6.2).

In the following sections, we first present the related work for rectilinear partitioning as well as application use cases in Section 2. Next, we present the preliminaries and our formulation of RPP in Section 3. Then in Section 4, we present the SGORP algorithm. Section 5 demonstrates how to use SGORP to solve different variants possibly motivated by real-world use-cases. Finally, Section 6 presents the detailed experimental evaluation, and in Section 7 we conclude.

2 RELATED WORK

2.1 Rectilinear Partitioning

Rectilinear partitioning (a.k.a., generalized block distribution) is a well studied problem [1, 12, 19, 24, 28]. Two of the existing important algorithms that we cover in the context of this paper for the (symmetric) rectilinear partitioning problem are Nicol’s algorithm [28] for 2-dimensional RPP and the PAL algorithm [38] for the 2-dimensional SRPP. The biggest difference between these methods and SGORP is that SGORP can work in an arbitrary number of dimensions and contains the 2-dimensional RPP and SRPP as special cases, while the other algorithms only work for their

individual cases. Nicol’s algorithm is an iterative method and uses the fact that given the partition of a dimension, it is possible to find the optimal partition for the other dimension. Compared to the Nicol’s algorithm, our method changes the partitions for all the dimensions at the same time in a single step. On the other hand, PAL algorithm is a single shot heuristic. It makes a single pass over the matrix nonzeros and partitions the matrix along the way. While the output partitions for both Nicol’s algorithm and PAL algorithm are at local optima, which was defined in (9), we will observe that SGORP will output partitions that are usually at better local optima.

Aspvall et al. [1] show that in the existence of heavy rows/columns, Nicol’s algorithm [28] focuses on heavy rows/columns, and that causes accumulation of the load in other rows. To overcome this problem, Aspvall et al. [1] propose an objective function which ignores the heavy rows/columns and solves the problem by iterating only 2-3 times.

Khanna et al. [19] and Gaur et al. [12] propose mapping rectilinear partitioning problem to the rectangle stabbing problem. The main drawback of this approach is its rather high computational complexity. In this process, the first stage involves finding all the rectangles that have higher load than a given target load, and it can take up to $O(n^4)$ for $n \times n$ dense matrices and $O(o^2)$ for sparse matrices with o nonzeros. Furthermore, rectangle stabbing algorithms running on these rectangles have a long runtime. Thus, we don’t compare SGORP with this class of algorithms.

There exists an iterative 4-approximation algorithm [26]. In this approach, the authors maintain costs for each individual row and column initialized to 1 at the start. After, at each step, they find a tile exceeding a given target load and scale the row and column costs of that tile by $1 + \frac{\epsilon}{2}$, where $\epsilon > 0$. Then, they partition the row and column cost arrays using the approach we describe in 4.1. One main difference between this algorithm and SGORP is that their algorithm requires a target load L^t as an input to see whether a partition exists whose maximum load is less than L^t , thus being a solution to a decision problem, whereas SGORP outputs the best partition found at the end. The other difference is that SGORP utilizes information that comes from every part of the load matrix and also their magnitudes, however its counterpart only utilizes the information about the location of the maximally loaded part.

2.2 Triangle Counting

The triangle counting problem [16, 20, 39] seeks to find mutually connected 3-vertices in an undirected graph. This is a crucial graph kernel that serves as a building block for many other graph problems. For the interest of this paper, recently, Hu et al. [16] proposed to use rectilinear partitioning to divide the computation among GPUs and Yaşar et al. [39] proposed a block-based triangle counting formulation using symmetric rectilinear partitioning to make the algorithm suitable for task-based execution on shared and distributed-memory systems. Both approaches try to minimize the maximum load of a partition. In this work, we show that SGORP can model this partitioning problem in a three dimensional space and optimize a different objective function successfully (see Section 5.4).

2.3 SUMMA-SpGEMM

SpGEMM, sparse matrix matrix multiplication, computes matrix multiplication on two sparse matrices. It is commonly used in graph applications, such as link prediction [25, 32], graph compression[27], and used in scientific computations [22, 31]. Due to its high complexity, and extreme irregularity, there has been an interest in optimizing SpGEMM [5, 9, 10, 21, 23] in both shared memory and distributed systems. SUMMA-SpGEMM[5], inspired by the original dense SUMMA [36], is one of the most commonly used technique for distributed memory systems. In SUMMA, the result matrix’s computation is partitioned rectilinearly, and each processor in a 2D virtual processor grid calculates a part. By iteratively generating partial results, space usage

for each process is limited to a constant number of parts of matrices. We show that SGORP can directly partition both input matrices simultaneously while incorporating minimization of the communication volume into partitioning objective (see Section 5.3).

3 PRELIMINARIES

3.1 Definitions

Rectilinear partitioning in the d -dimensional space consists of d 1-dimensional partitions, one for each of the d -dimensions. That's why we will start by defining what it means to partition a 1-dimensional interval.

Given an interval $r = [a, b)$, a partitioning p of r into k parts is an array $[p[0], \dots, p[k]]$ such that $p[0] = a$, $p[k] = b$ and it is monotonic, i.e., $p[j] \leq p[j+1], \forall j \in [k]$. Here, we use $[k]$ to represent $\{0, \dots, k-1\}$ and will use $[k]^+$ to represent $\{1, \dots, k\}$.

Next, we will define the objects that we will try to partition. Let us define a load distribution as an integrable function $f : \mathbb{R}^d \rightarrow \mathbb{R}^+$, and let us define its load $L(f)$ as:

$$L(f) = \int_{-\infty}^{\infty} \dots \int_{-\infty}^{\infty} f(x_1, \dots, x_d) dx_d \dots dx_1 < \infty.$$

Given a d -dimensional load distribution f , we would like to find $p = (p_1, \dots, p_d)$ such that each p_i is a partitioning of \mathbb{R} into k_i parts. Together, the p_i 's imply a partitioning of the whole space \mathbb{R}^d into $k = (k_1, \dots, k_d)$ parts. Our goal is to minimize $L(f, p)$, the maximum of loads of these parts, i.e.,

$$L^* = \min_{p=(p_1, \dots, p_d)} L(f, p) \quad (1)$$

$$L(f, p) = \max_{j \in [k_1] \times \dots \times [k_d]} L(f, p, j) \quad (2)$$

$$L(f, p, j) = \int_{p_1[j_1]}^{p_1[j_1+1]} \dots \int_{p_d[j_d]}^{p_d[j_d+1]} f(x_1, \dots, x_d) dx_d \dots dx_1 \quad (3)$$

Note that, we seek a $p = (p_1, \dots, p_d)$ to minimize $L(f, p)$, the load of the maximally loaded part. And finally, let us also define the prefix sum $F : \mathbb{R}^d \rightarrow \mathbb{R}^+$ of f as

$$F(x_1, \dots, x_d) = L(f, [-\infty, x_1], \dots, [-\infty, x_d])$$

and the prefix sum in the i -th dimension $F_i : \mathbb{R} \rightarrow \mathbb{R}^+$ as

$$F_i(x) = F(x_1, \dots, x_d) : x_i = x \text{ and } x_j = \infty, \forall j \neq i.$$

Let us denote the inverse of the prefix sum in the i -th dimension as F_i^{-1} . We will use these prefix sums in the next section to reparametrize partitions of each of the d dimensions and it will serve as the basic building block of our method. A summary of used notation can be found in Table 1.

3.2 Modeling sparse tensors and point datasets as load distributions

Let A be a d -dimensional sparse tensor with o nonzeros defined via an ordered index set, $A_I \in \mathbb{N}^{o \times d}$, and corresponding values of these indices, $A_V \in \mathbb{R}^o$. Thus:

$$A[A_I[i]] = A_V[i], \forall i$$

$$A[e] = 0, \forall e \in \mathbb{N}^d \setminus A_I$$

Note that, a sparse tensor A is essentially a function from the index space \mathbb{N}^d to the value space \mathbb{R} , i.e., $A : \mathbb{N}^d \rightarrow \mathbb{R}$, and it is zero for any index not in the index set.

Table 1. Notation used in this paper.

| Symbol | Description |
|-------------------------------|--|
| $[k]$ | Integer set: $\{0, \dots, k-1\}$ |
| $[k]^+$ | Integer set: $\{1, \dots, k\}$ |
| $[a, b)$ | Real interval: $\{x \in \mathbb{R} : a \leq x < b\}$ |
| $p = (p_1, \dots, p_d)$ | A partitioning of \mathbb{R}^d , where p_i is the partition array in i -th dimension |
| $k = (k_1, \dots, k_d)$ | Nu. of parts in each dimension of p |
| $L(f, p, j)$ | Load at index $j = (j_1, \dots, j_d)$ with p |
| $L(f, p)$ | Maximum load |
| $F_i(x)$ | Prefix sum: i -th dimension, point x |
| $F_i^{-1}(x)$ | Inverse of F_i at point x |
| A | A sparse tensor |
| f_A | Load distribution of the tensor A |
| $\pi = (\pi_1, \dots, \pi_d)$ | Parametrization of $p = (p_1, \dots, p_d)$ |
| $g = (g_1, \dots, g_d)$ | Subgradient at the current parameters |
| $\eta(t)$ | Step size depending on iteration t |

In the case of a given d -dimensional dataset with o points, we can treat $A_I \in \mathbb{R}^{o \times d}$ as the coordinates of the points and $A_V \in \mathbb{R}^o$ as their weights. As there isn't a fundamental difference between sparse tensors and point datasets in this sense, we will talk about datasets as sparse tensors.

Given a d -dimensional sparse tensor A , we will define the corresponding d -dimensional load distribution f_A as follows:

$$f_A(x_1, \dots, x_d) = \sum_{u \in A_I} \delta(x - u)A[u], \quad (4)$$

where $\delta : \mathbb{R}^d \rightarrow \mathbb{R}$ denotes the Dirac delta function to model a point-wise load that a nonzero in A implies. Defined this way, f represents the distribution of the nonzeros of A in \mathbb{R}^d . In the scenario where the values of the nonzeros of A don't matter, we assume that all the values are set to 1.

4 SGORP: SUBGRADIENT OPTIMIZATION FOR RECTILINEAR PARTITIONING

In this section, we explain our customizable framework, SGORP. The reason we are classifying our method under Subgradient Optimization [34] is that; we don't have access to the gradient of our objective function. We pick a direction to move our parameters that will probably improve the objective but might not every iteration. Given a d -dimensional load distribution f , SGORP partitions the load distribution, f , while also taking any user given equality constraints on the partition vectors of different dimensions to solve the symmetric RPP. In the following subsections, we first explain how the algorithm works for the 1-dimensional partitioning problem. Afterwards, we show how to generalize our approach to the multi-dimensional case. Then, we show how we can incorporate equality constraints on the partition vectors of different dimensions into our framework and how to initialize the optimization variables. Since SGORP is an iterative method, we also discuss possible stopping conditions and step size rules. Finally, we give an overall summary of our method and illustrate a single iteration on a toy example.

4.1 1-dimensional partitioning problem

We first consider the 1-dimensional partitioning problem to build up an intuition for the RPP. Let f be a 1-dimensional load distribution. Our goal is to find a way, $p = (p_1)$, to partition it into $k = (k_1)$ parts while minimizing $L(f, p)$. Given our objective, there exists a partition $p^* = (p_1^*)$ such that

$L(f, p^*) = \frac{L(f)}{k_1}$. Note that F is differentiable by definition, and so it is also continuous. We can also explicitly express the entries of p_1^* as follows:

$$p_1^*[j] = F_1^{-1}\left(j \frac{L(f)}{k_1}\right), \forall j \in [k_1 + 1]$$

Unfortunately, we can not determine the optimal solution p^* explicitly using this formulation for higher-dimensional problems. Therefore for a given p , we seek a way to compute its subgradient to improve it iteratively. As one can notice, F_1^{-1} plays a crucial role to solve the 1-dimensional partitioning problem. Thus, we argue that in the multidimensional case, it might also be beneficial to parametrize p with $\pi = (\pi_1, \dots, \pi_d)$ as follows:

$$p_i[j] = F_i^{-1}(\pi_i[j])$$

In this parametrization, the optimal solution for the 1-dimensional case $\pi^* = (\pi_1^*)$ can be expressed as:

$$\pi_1^*[j] = j \frac{L(f)}{k_1}$$

Then we define the load, L_π , as:

$$L_\pi(f, \pi) = \max_{j \in [k_1] \times \dots \times [k_d]} L_\pi(f, \pi, j) \quad (5)$$

$$L_\pi(f, \pi, j) = L(f, (F_1^{-1}(\pi_1), \dots, F_d^{-1}(\pi_d)), j) \quad (6)$$

Finally, the subgradient $g = (g_1)$ for the 1-dimensional case can be written as:

$$g_1[j] = \frac{\partial L_\pi(f, \pi)}{\partial \pi_1} = \pi_1[j] - \pi_1^*[j]$$

and the update rule with step size $\eta(t) > 0$ at iteration t as:

$$\pi' = \pi - \eta(t)g \quad (7)$$

Note that when $\eta = 1$, we achieve the optimal solution in one step.

4.2 Multidimensional partitioning problem

Let f be a d -dimensional load distribution and say we want to partition it into $k = (k_1, \dots, k_d)$ parts. We aim to find a good way to define the subgradient $g = (g_1, \dots, g_d)$ so that applying the update rule in (7) repeatedly, we will get closer and closer to local optima. But before that, let us define $r_i(f, \pi)[j_i]$ as the maximum over all dimensions except the i th one as follows:

$$r_i(f, \pi)[j_i] = \max_{j \in [k_1] \times \dots \times \{j_i\} \times \dots \times [k_d]} L_\pi(f, \pi, j), \forall j_i \in [k_i] \quad (8)$$

We claim that a given π is at local optima in the sense that changing any of the π_i while keeping others fixed will increase the value of $L(f, \pi)$ when the following holds:

$$r_i(f, \pi)[j_i] = L_\pi(f, \pi), \forall i, j_i$$

Thus, the optimal solution π^* lies in the set

$$S = \{\pi \mid r_i(f, \pi)[j_i] = L_\pi(f, \pi), \forall i, j_i\} \quad (9)$$

In the 1-dimensional case, this set only has a single member, and it is the optimal solution. However, in the multidimensional case, this set is not necessarily a singleton.

We will define the subgradient $g = (g_1, \dots, g_d)$ as follows:

$$g_i[j_i] = \sum_{u=0}^{j_i-1} r_i[u] - \frac{j_i}{k_i} \sum_{u=0}^{k_i-1} r_i[u], \forall i, j_i \quad (10)$$

so that a given π will get closer and closer to the set S by applying our update rule repeatedly. Let's verify if the subgradient g becomes 0 when $\pi \in S$:

$$\begin{aligned} g_i[j_i] &= \sum_{u=0}^{j_i-1} r_i[u] - \frac{j_i}{k_i} \sum_{u=0}^{k_i-1} r_i[u] \\ &= \sum_{u=0}^{j_i-1} L_\pi(f, \pi) - \frac{j_i}{k_i} \sum_{u=0}^{k_i-1} L_\pi(f, \pi) \\ &= j_i L_\pi(f, \pi) - j_i L_\pi(f, \pi) = 0 \end{aligned}$$

Indeed, g becomes 0 when π is at a local optima as expected.

Note that, our update rule in (7) reads the same for each of the d dimensions:

$$\pi'_i = \pi_i - \eta_i(t)g_i, \forall i \quad (11)$$

Again to verify, in the 1-dimensional case, we have:

$$\begin{aligned} \pi'_1[j_1] &= \pi_1[j_1] - \eta g_1[j_1] \\ &= \pi_1[j_1] - \eta \sum_{u=0}^{j_1-1} r_1[u] + \eta \frac{j_1}{k_1} \sum_{u=0}^{k_1-1} r_1[u] \\ &= \pi_1[j_1] - \eta \sum_{u=0}^{j_1-1} (\pi_1[u+1] - \pi_1[u]) \\ &\quad + \eta \frac{j_1}{k_1} \sum_{u=0}^{k_1-1} (\pi_1[u+1] - \pi_1[u]) \\ &= \pi_1[j_1] - \eta(\pi_1[j_1] - \pi_1[0]) + \eta \frac{j_1}{k_1} (\pi_1[k_1] - \pi_1[0]) \\ &= \pi_1[j_1] - \eta(\pi_1[j_1] - 0) + \eta \frac{j_1}{k_1} (L(f) - 0) \\ &= \pi_1[j_1] - \eta(\pi_1[j_1] - \frac{j_1}{k_1} L(f)) \\ &= \pi_1[j_1] - \eta(\pi_1[j_1] - \pi_1^*[j_1]) \end{aligned}$$

4.3 Constrained optimization

Again, let f be a d -dimensional load distribution and say we want to again partition it into $k = (k_1, \dots, k_d)$ parts. This time however, we will have equality constraints among the partitions, e.g., $p_1 = p_2 = p_3$ and $p_4 = p_d$, etc. Let's say we group the dimensions whose partitions are constrained to be equal and we are left with only \hat{d} groups. Then, we can encode these constraints as:

$$\begin{aligned} p_i &= \hat{p}_{\hat{i}}, \text{ for some } \hat{i} \in [\hat{d}]^+ \\ C_{\hat{i}} &= \{i \mid p_i = \hat{p}_{\hat{i}}\} \end{aligned}$$

If we optimize over \hat{p} , then the problem turns into an unconstrained one. However, first we need to find a way to parametrize \hat{p} as $\hat{\pi}$ in a similar manner to our former discussion. First, we define $\hat{F}_{\hat{i}}(x)$ as:

$$\hat{F}_{\hat{i}}(x_{\hat{i}}) = \frac{1}{|C_{\hat{i}}|} \sum_{i \in C_{\hat{i}}} F_i(x_i)$$

With this, we parametrize \hat{p} as $\hat{\pi}$ as in the previous section:

$$\hat{p}_i[j_i] = \hat{F}_i^{-1}(\hat{\pi}_i[j_i])$$

As is the case with p_i and \hat{p}_i , we will define π_i as an alias to the corresponding $\hat{\pi}_i$. In a similar manner, we can define $\hat{r}_i(f, \hat{\pi})[j_i]$ as:

$$\hat{r}_i(f, \hat{\pi})[j_i] = \max_{\forall i \in C_i} r_i(f, \pi)[j_i] \quad (12)$$

and finally, we can define the subgradient, again, the same as in the previous section:

$$\hat{g}_i[j_i] = \sum_{u=0}^{j_i-1} \hat{r}_i[u] - \frac{j_i}{k_i} \sum_{u=0}^{k_i-1} \hat{r}_i[u], \forall i, j_i \quad (13)$$

4.4 Initializing $\hat{\pi}$

The possible values for $\hat{\pi}_i[j_i]$ lie in the range of \hat{F}_i . Since \hat{F}_i is a monotonic function and $\hat{F}_i(-\infty) = 0$ and $\hat{F}_i(\infty) = L(f)$ for all \hat{i} , we could choose to deterministically initialize $\hat{\pi}_i[j_i]$ as:

$$\hat{\pi}_i[j_i] = \frac{j_i}{k_i} L(f).$$

Another option to initialize $\hat{\pi}_i[j_i]$ is to use the uniform distribution with range $(0, L(f))$. Note that $\hat{\pi}_i$ has to be monotonic so we sort $\hat{\pi}_i$ after initializing them with the uniform distribution. After this, we set $\hat{\pi}_i[0] = 0$ and $\hat{\pi}_i[k_i] = L(f)$. This way of initialization is better because we suspect that d -dimensional rectilinear partitioning for any $d \geq 2$ and any types of constraints is NP-hard. Thus, it is expected that there are many local optima. Random initialization makes it so that multiple runs of the algorithm with different random seeds produce different outputs which can be considered to be a good property since a single run might get stuck at a bad local optima.

4.5 Stopping condition

Since we have characterized the optimal solution to be in the set S defined in (9), this immediately gives us a metric to decide when to stop. Since the following holds

$$L_\pi(f, \pi) = \max_{j_i} \hat{r}_i(f, \hat{\pi})[j_i], \forall \hat{i}$$

we can measure for all \hat{i} how close $r_i(f, \hat{\pi})$ is to the uniform distribution when we consider $r_i(f, \hat{\pi})$ as an unnormalized probability distribution. This can be done using norms, including L_1 , L_2 or even L_∞ . During the iterations, we can check whether it is close enough and if so, we can choose to terminate the algorithm. Among all of the available options, we choose to stop the algorithm when the following holds:

$$\frac{L_\pi(f, \pi) - \min_{i, j_i} \hat{r}_i[j_i]}{\min_{i, j_i} \hat{r}_i[j_i]} < \epsilon \quad (14)$$

However, when we represent sparse tensors as load distributions, the load function that we defined in (3) won't be continuous. Thus, it might be impossible for $\hat{r}_i(f, \hat{\pi})$ to approximate an unnormalized uniform probability distribution causing the algorithm to never stop. Therefore, we resort to the following technique: for $c \sum_{i=1}^d k_i$ iterations after the last update of the best solution found so far, if the solution quality doesn't improve more than a factor of $1+\epsilon$, then SGORP stops. Our experimental results show that combining this technique with the aforementioned stopping condition gives good results with $c = 10$ and $\epsilon = 0.001$.

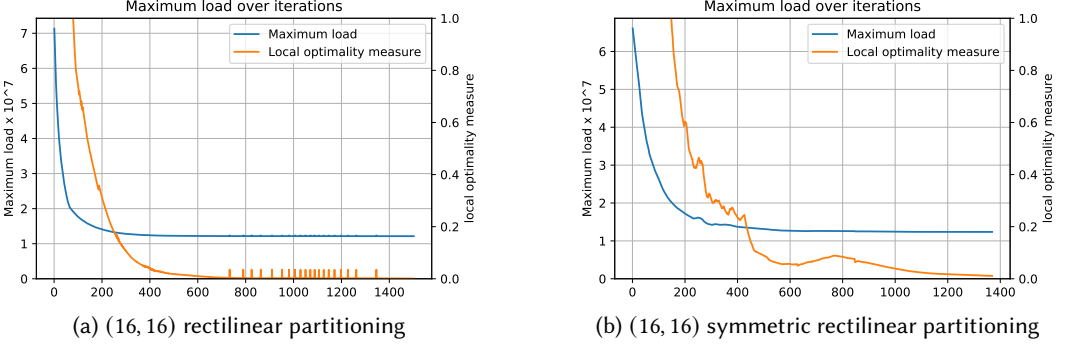


Fig. 1. Plots of $L(f, \pi)$ and closeness to local optimality with respect to iteration number on twitter7 matrix from SuiteSparse with (16, 16) partitioning.

In Figure 1, if the orange curve gets sufficiently close to 0, then we can stop because we have reached a local optima. We can also choose to stop when the blue curve starts to flatten in case we can't get close enough to a local optima. In Figure 1b, we observe that both the blue and orange curves are less smooth compared to Figure 1a. Our explanation for this phenomenon is that the parameters of partition arrays of both dimensions are shared in the symmetric case, so the effect of the first and the second dimensions to the subgradient sometimes conflict each other. At those times, SGORP might move $\hat{\pi}$ further away from the set S defined in (9). Another reason for non-smoothness is that the object we are partitioning is discrete in nature. That is why there are some jumps at the end of the blue and orange curves in Figure 1a.

4.6 Step size selection

The update rule we defined in (11) depends on current iteration t . There is a multitude of step size rules that can be used one of which is the constant step size rule [4]. However, we choose to use a diminishing step size rule, specifically $\eta_i(t) \approx \frac{\mu}{\sqrt{\frac{t}{k_i} + T}}$, where $\mu = 1$ and $T = 100$ were determined to work well empirically in our experiments.

4.7 Overall summary and an example

Algorithm 1 presents the pseudocode of our proposed method SGORP. First, we initialize the partitioning variables $\hat{\pi}$. Then, in each step, SGORP computes the subgradients \hat{g}_i and updates $\hat{\pi}$, and keeps track of the best solution found so far, $\hat{\pi}^*$. SGORP returns the best solution when the stopping condition is achieved.

As a toy example, given the partitioned matrix A in Figure 2a as our initial state with partitioning (p, p) , where $p = [0, 2, 4, 8]$, we apply a single update of our algorithm when there are no constraints. Since A is a sparse matrix, we first get its load distribution f_A . Note that $L(f_A, (p, p)) = 5$. After that, we compute the prefix sums F_1 and F_2 by counting the numbers of nonzeros along the rows and columns to get $F_1 = [0, 5, 9, 11, 11, 12, 12, 14, 15]$ and $F_2 = [0, 2, 3, 4, 7, 8, 9, 13, 15]$. By plugging p into F_1 and F_2 as an index, we get $\pi_1 = [F_1[p[0]], F_1[p[1]], F_1[p[2]], F_1[p[3]]] = [0, 9, 11, 15]$ and $\pi_2 = [F_2[p[0]], F_2[p[1]], F_2[p[2]], F_2[p[3]]] = [0, 3, 7, 15]$. We also compute the loads of each part to get $[[2, 2, 5], [0, 2, 0], [1, 0, 3]]$. As the next step, we compute $r_1 = [5, 2, 3]$ and $r_2 = [2, 2, 5]$. After that, we compute the subgradients $g_1 = [0, \frac{5}{3}, \frac{1}{3}, 0]$ and $g_2 = [0, 1, -1, 0]$. If we have the step size $\eta = 2$, then updated parameters become $\pi_1 = [0, \frac{17}{3}, \frac{31}{3}, 15]$ and $\pi_2 = [0, 5, 11, 15]$. Doing binary

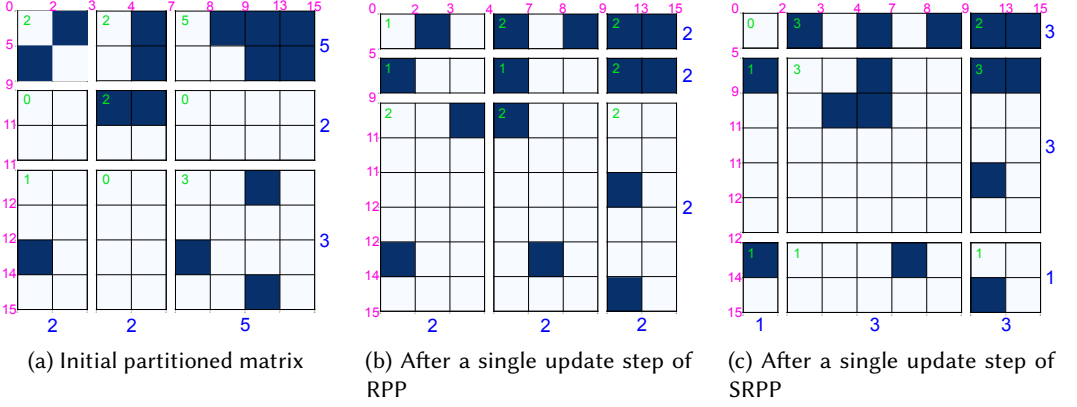


Fig. 2. A toy matrix partitioned in various ways. The (magenta) numbers to the left and top of the figures denote the prefix sums F_1 and F_2 . The (blue) numbers to the right and bottom represent the maximum loads r_1 and r_2 . Finally, the (green) numbers inside the boxes show the load of the part they are in.

Algorithm 1: SGORP(f, C, k)

▶ f : A d -dimensional load distribution
 ▶ C : Set of constraints
 ▶ $k = (k_1, \dots, k_d)$: Partition vector sizes of each dimension

- 1 $\hat{\pi} = \text{INITIALIZE}()$ ▶ See Section 4.4
- 2 $\hat{\pi}^* = \hat{\pi}$ ▶ Initialize best solution found so far
- 3 $t = 0$ ▶ Initialize iteration count to 0
- ▶ See Section 4.5 for the stopping condition
- 4 **while not** (14) **do**
- 5 Compute r_i using (8), \hat{r}_i using (12), and \hat{g}_i using (13)
- 6 $\hat{\pi}_i = \hat{\pi}_i - \eta_i(t)\hat{g}_i$ st. $\hat{i} \in [d]^+$
- 7 **if** $L(f, \hat{\pi}) < L(f, \hat{\pi}^*)$ **then**
- 8 $\hat{\pi}^* = \hat{\pi}$ ▶ Best solution improved
- 9 $t = t + 1$
- 10 **return** $\hat{\pi}^*$

searches in F_1 and F_2 to compute F_1^{-1} and F_2^{-1} , we get the new partition vectors $p_1 = [0, 1, 2, 8]$ and $p_2 = [0, 3, 6, 8]$. With this new partition of the matrix, we have $L(f_A, (p_1, p_2)) = 2$, down from 5.

Now we show a single step of our algorithm when there is an equality constraint along the matrix rows and columns. In this case, we compute $\hat{F}_1 = \frac{F_1 + F_2}{2} = [0, \frac{7}{2}, 6, \frac{15}{2}, 9, 10, \frac{21}{2}, \frac{27}{2}, 15]$. By looking-up each element of p in \hat{F}_1 , we get $\hat{\pi}_1 = [0, 6, 9, 15]$. Since we already computed r_1 and r_2 above, we can compute $\hat{r}_1 = [5, 2, 5]$ by taking an element-wise max of r_1 and r_2 . After that, we compute the subgradient $\hat{g}_1 = [0, 1, -1, 0]$. Using $\eta = 2$, we get updated $\hat{\pi} = [0, 4, 11, 15]$. Doing binary searches on \hat{F}_1 , we get the new partition vector $\hat{p}_1 = [0, 1, 6, 8]$. Because of the constraint $p_1 = \hat{p}_1 = p_2$, we have $L(f_A, (p_1, p_2)) = 3$, down from 5.

5 MAPPING PARTITIONING PROBLEMS INTO SGORP

In this section, we propose modeling strategies to map four different applications into SGORP. The first two of these applications model the partitioning problem using two-dimensional objective functions, while the last two of these applications use three-dimensional objective functions.

5.1 2-dimensional RPP

Nicol's [28] rectilinear partitioning algorithm partitions a given sparse matrix A into (k_1, k_2) parts and tries to minimize the maximum number of nonzeros contained in the most loaded partition. SGORP can achieve the same type of partitioning: Given a 2-dimensional sparse matrix A , we treat it as a 2-dimensional load distribution f_A as in (4). The objective is to partition f_A into (k_1, k_2) parts. Thus, this use of our framework is a direct contender to Nicol's algorithm, which we will investigate in the experiments section. We will refer to this variant of SGORP as SGO-2DR. In short, we will have SGORP solve the following optimization problem:

$$\min_{p_1, p_2} \max_{j_1, j_2} L(f_A, (p_1, p_2), (j_1, j_2)) \quad (15)$$

5.2 2-dimensional SRPP

The partitioning algorithms presented in [38] partition a given sparse matrix A into (k, k) parts resulting in partition vectors (p, p) while minimizing the maximum number of nonzeros contained in a single partition. Note that the use of p for the partition vectors of both dimensions implies an equality constraint, as explained in Section 4.3. The objective is to partition f_A into (k, k) parts. This kind of use of our framework is a direct contender to the algorithms presented in [38]. In our experiments, we compare SGORP with the PAL algorithm implemented in that library. We will refer to this variant of SGORP as SGO-2DS. In short, SGORP solves the following optimization problem:

$$\min_{p_1=p_2} \max_{j_1, j_2} L(f_A, (p_1, p_2), (j_1, j_2)) \quad (16)$$

5.3 3-dimensional RPP Use Case: SpGEMM

SGORP is a flexible framework, and it can optimize different objective functions. This property is highly useful for modeling a wide range of applications. For instance, for the Sparse Matrix-Matrix Multiplication (SpGEMM) kernel that uses the SUMMA algorithm, one might want to minimize the maximum communication volume during each communication round. In this algorithm, each processor (u, v) in a $k \times k$ processor grid multiplies the tile (u, w) of A with the tile (w, v) of B and adds it to the tile (u, v) of C in communication round w . The total volume of communication done by the processor (u, v) in round w is the sum of the load of the tile (u, w) of A and the tile (w, v) of B . The goal is to minimize the maximum total volume of communication in the round w between all processors, i.e. $\max_{u,v} \text{nnz}(A[u, w]) + \text{nnz}(B[w, v])$. When we consider all of the communication rounds, the objective becomes to minimize $\sum_w \max_{u,v} \text{nnz}(A[u, w]) + \text{nnz}(B[w, v])$. However, it is not possible to optimize this objective function with our framework as subgradients vanish when we sum over a dimension. That is why we choose to minimize $\max_{u,w,v} \text{nnz}(A[u, w]) + \text{nnz}(B[w, v])$.

To map this problem into our framework, let f_A and f_B be 2-dimensional load distributions representing matrices A and B as in Section 3.2. Let $f(x_1, x_2, x_3) = f_A(x_1, x_2) + f_B(x_2, x_3)$. Note that f is 3-dimensional load distribution. Solving the problem of partitioning f into (k, k, k) parts and getting the resulting partitions (p_1, p_2, p_3) , directly corresponds to minimize the communication volume of the Sparse SUMMA algorithm where A is distributed with respect to (p_1, p_2) and B is

distributed with respect to (p_2, p_3) . In short, SGORP solves the following optimization problem:

$$\min_{p_1, p_2, p_3} \max_{j_1, j_2, j_3} L(f, (p_1, p_2, p_3), (j_1, j_2, j_3)) \quad (17)$$

We will refer to this variant of SGORP as SGO-3DR.

5.4 3-dimensional SRPP Use Case: Triangle Count

Triangle Counting Problem [16, 39] can be another use-case. When we partition the adjacency matrix of a given graph using a symmetric-rectilinear fashion, edges of a triangle can appear in at most three of the partitions. Furthermore, in a triangle, for chosen two edges, there exists only one sub-graph such that the third edge belongs. If one partitions the adjacency matrix A into (k, k) parts using a partition p_1, p_2 under the constraint $p_1 = p_2$, then there will be $\approx k^3$ instances (i.e., tasks) of the triangle counting problem, each seeks triangles in $(A[u, w], A[w, v], A[u, v])$. In the heterogeneous environment, where the memory of the co-processors or the bandwidth between the host-processor and the co-processors are limited, $nnz(A[u, w]) + nnz(A[w, v]) + nnz(A[u, v])$ of task (u, w, v) will correspond to transfer times to the co-processors and the memory requirement. Thus, the objective is to minimize $\max_{u, w, v} nnz(A[u, w]) + nnz(A[w, v]) + nnz(A[u, v])$.

To map this problem into our framework, let f_A be a 2-dimensional load distribution representing the adjacency matrix A and let $f(x_1, x_2, x_3) = f_A(x_1, x_2) + f_A(x_2, x_3) + f_A(x_1, x_3)$. Solving the problem of partitioning f using (p_1, p_2, p_3) into (k, k, k) parts with the constraint $p_1 = p_2 = p_3$, directly corresponds to minimize the maximum communication cost of a processor. We will refer to this variant of SGORP as SGO-3DS. In short, SGORP solves the following optimization problem:

$$\min_{p_1=p_2=p_3} \max_{j_1, j_2, j_3} L(f, (p_1, p_2, p_3), (j_1, j_2, j_3)) \quad (18)$$

6 EXPERIMENTS

In this section, we compare the performance of our proposed algorithms (SGO-2DS, SGO-2DR, SGO-3DR, SGO-3DS) with state-of-the-art rectilinear and symmetric rectilinear partitioning algorithms. We use Nicol's (NIC) [28], Aspvall et al.'s (2SWP) [1] and Muthukrishnan and Suel's (4APX) [26] rectilinear partitioning algorithms for the nonsymmetric case and Probe a Load (PAL) symmetric rectilinear partitioning algorithm for the symmetric case. We use NIC and PAL with their default parameters from the SARMA library [38]. We choose to use a maximum iteration limit of 10000 for the 4APX algorithm with $\epsilon = 0.01$. For the 4APX algorithm, the authors state in their paper that the number of iterations required to converge is on the order of $O(k_1 \log N)$, where k_1 stands for the number of parts in a dimension and N stands for the maximum dimension of the input matrix. We also include uniform partitioning (UNI) in our experiments as the baseline. Note that SGO-2DS and SGO-3DS output symmetric partitions whereas SGO-2DR and SGO-3DR output rectilinear partitions.

SGORP variants use the random initialization as explained in Section 4.4. To reduce the variance caused by randomness, the median result of 10 runs is taken in all reported results.

We ran all of the experiments on the Hive cluster of Georgia Tech. Hive has 416 compute nodes, each is equipped with 2×2.7 GHz Intel Xeon 6226 CPUs (with 12-cores), and 192 GB of RAM. Interconnection network is EDR Infiniband (100Gbps). Each algorithm run had a single such node with all 24 cores for their use.

All of the sparse matrices used in our experiments were downloaded from the SuiteSparse Matrix Collection [8]. We excluded non-square matrices and matrices with less than 10^6 or more than 2×10^9 nonzeros. By the time of this experimentation there were 687 matrices, out of 2856, that fit our criteria.

We downloaded 17 additional point datasets from the DIMACS10 workshop repository [7]; Street Networks, and Frames from 2D Dynamic Simulations categories. The number of points in this dataset varies from 10^5 to 5×10^7 .

We present our results using performance profile plots [11]. In these plots, the y -axis denotes the relative number of test instances, and the x -axis denotes the ratio of the metric of interest to the best performing algorithm on one of the test instances. The higher and closer a plot is to the y -axis, the better the method is.

Furthermore, in order to support reproducibility, we provide normalized load imbalance (with respect to average non-zero per part) and absolute algorithm execution times for a subset of data in Appendix A.

6.1 Implementation

We have contributed our implementation of SGORP, the two-sweep (2SWP) algorithm in [1] and the four approximation (4APX) algorithm in [26] to the SARMA library and it is publicly available at <https://github.com/GT-TDAIab/SARMA> via a BSD-license. SARMA library is a suite of spatial partitioning algorithms implemented using C++17 and the parallel standard library using shared memory parallelism. We particularly used the sparse prefix sum data structure provided in SARMA to represent 2-dimensional load distributions f_A implied by the sparse matrices A used during experiments. Given a sparse matrix A of dimensions (m, n) with o nonzeros, this data structure enables us to query the load of a rectangular region in the 2-dimensional space in $O(\log n \log m)$ time using $O(o \log \min(m, n))$ space.

The computational complexity of our algorithm is given by sparse-prefix-sum data structure construction and load queries. SGORP can be computed in $O(o \log \min(m, n) + \tau k_1 k_2 \log n \log m)$ for the 2-dimensional case where τ stands for the number of iterations. Note that, while the number of iterations required depends on many factors, it is at most thousands in practice and it highly depends on the selected parameters for the stopping condition and the step size. The data structure construction dominates the complexity of our algorithm. However, one can reduce that by sparsifying the graph, that is, sampling the nonzeros of the input sparse-matrix [38].

6.2 Evaluation of the Partitioning Quality

In this sub-section, we compare the performance of our proposed algorithms with-respect-to state-of-the-art partitioning algorithms for given objective functions. Depending on the nature of the partitioning problem we use NIC, 4APX, 2SWP, PAL, and UNI algorithms as baselines. In the following experiments we present results for 8×8 , 16×16 , and 32×32 partitionings.

6.2.1 2-dimensional Rectilinear Partitioning. In this experiment, we compare SGO-2DR, and SGO-2DS with NIC, 4APX, 2SWP, PAL and UNI algorithms. In this experiment the objective function is minimizing the load of the maximum loaded partition. Note that comparing SRPP algorithms with RPP algorithms is not fair because SRPP algorithms have more constraints. However we include these algorithms in this experiment to give the reader an idea of how much of a limitation SRPP brings compared to RPP. Figure 3 illustrates that the relative order of the algorithms with respect to partitioning quality is SGO-2DR, NIC, 2SWP, SGO-2DS, PAL, 4APX and UNI. We see that the difference between SGO-2DR and NIC algorithms start to decrease as we increase the number of parts from $(8, 8)$ to $(32, 32)$. However, SGORP still outperforms NIC both in terms of partitioning quality and also execution time as we will present below. Since RPP algorithms can output different partition vectors for each dimension as opposed to SRPP algorithms, this kind of a difference was expected.

In the point datasets, we see that SGO-2DR and NIC are much closer, SGO-2DR outperforming NIC for the (8, 8) case and NIC outperforming SGO-2DR for the (32, 32) case in Figure 7. Note that, the number of instances is small, only 17. Thus, we believe that the use of sparse matrices gives a better picture of overall quality.

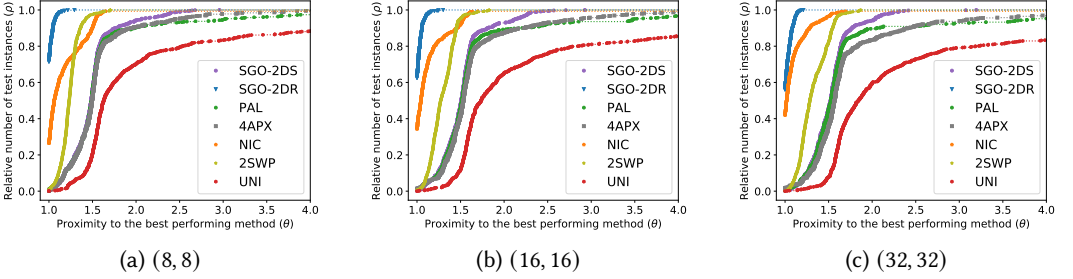


Fig. 3. Performance profile plots of the partitioning methods with natural reordering. The algorithms are compared wrt. (15).

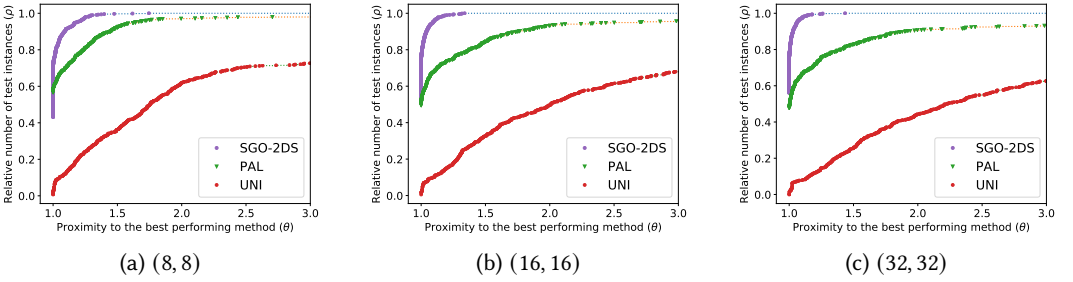


Fig. 4. Performance profile plots of the symmetric partitioning methods when the graphs are reordered in ascending order of their degrees and only the upper triangular part is kept. The algorithms are compared wrt. (16).

6.2.2 2-dimensional Symmetric Rectilinear Partitioning. In this experiment, we compare SGO-2DS, PAL and UNI algorithms. The objective function tries to minimize the load of the maximum loaded partition. As illustrated in Figure 4, we see that the relative order of the algorithms with respect to partitioning quality is SGO-2DS, PAL and UNI. We observe that the difference between SGO-2DS and PAL algorithms increases proportional to the number of parts, from (8, 8) to (32, 32). We also observe that on nearly 80% of the matrices, the partition quality is very close between SGO-2DS and PAL algorithms while SGO-2DS outperforms the PAL algorithm on the rest of the matrices. Therefore we claim that SGO-2DS is more resistant to the sparsity pattern of the given matrix and outputs better partitions. As expected, the UNI algorithm performs really badly and it gives up to 3 times worse partitions.

6.2.3 3-dimensional Rectilinear Partitioning. In this experiment, we compare SGO-3DR, SGO-2DS, NIC, PAL and UNI algorithms and we use (17) as the objective function. In this use case, we require 3 partition arrays $p = (p_1, p_2, p_3)$. For the symmetric methods (SGO-2DS, PAL and UNI) we use the same partition array for each dimension. However, for the NIC algorithm, initially, we partition the first load distribution f_A to get p_1 and p_2 . Then we find the optimal p_3 to partition f_B when

the partition array for the first dimension of f_B is p_2 . SGO-3DR outputs 3 partition arrays as an output. Figure 5, shows that the relative order of the algorithms with respect to partitioning quality is SGO-3DR, NIC, SGO-2DS, PAL and UNI.

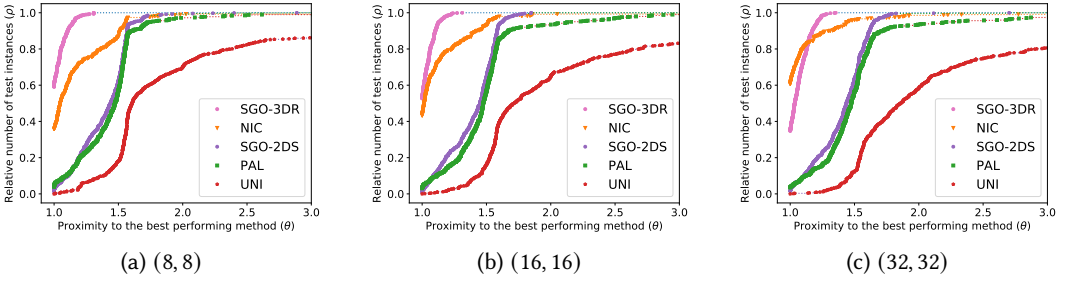


Fig. 5. Performance profile plots of the partitioning methods with natural reordering. The algorithms are compared wrt. (17).

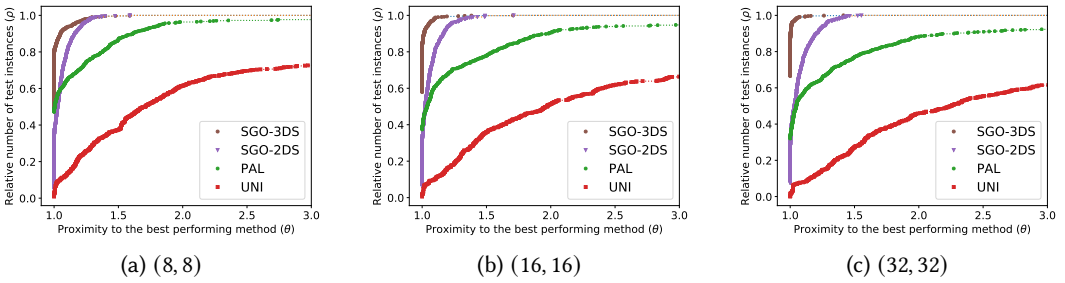


Fig. 6. Performance profile plots of the symmetric partitioning methods when the graphs are reordered in ascending order of their degrees and only the upper triangular part is kept which is useful when doing triangle counting. The algorithms are compared wrt. (18).

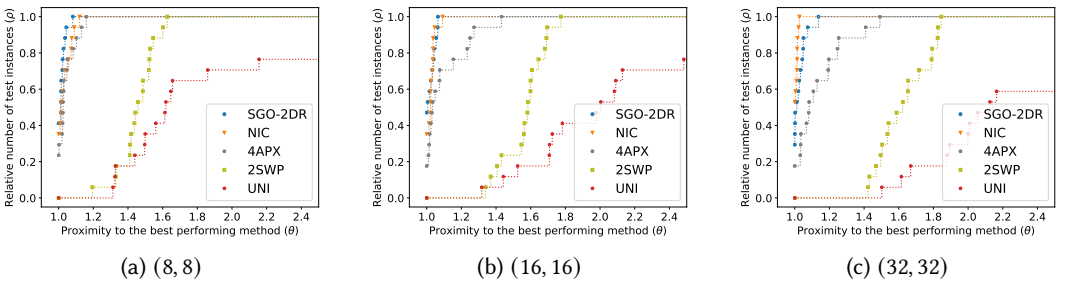


Fig. 7. Performance profile plots of the partitioning methods on point datasets. The algorithms are compared wrt. (15).

6.2.4 3-dimensional Symmetric Rectilinear Partitioning. In this experiment, we compare SGO-3DS, SGO-2DS, PAL and UNI algorithms, and we use (18) as the objective function. Figure 6 illustrates that the relative order of the algorithms with respect to partitioning quality is SGO-3DS, SGO-2DS,

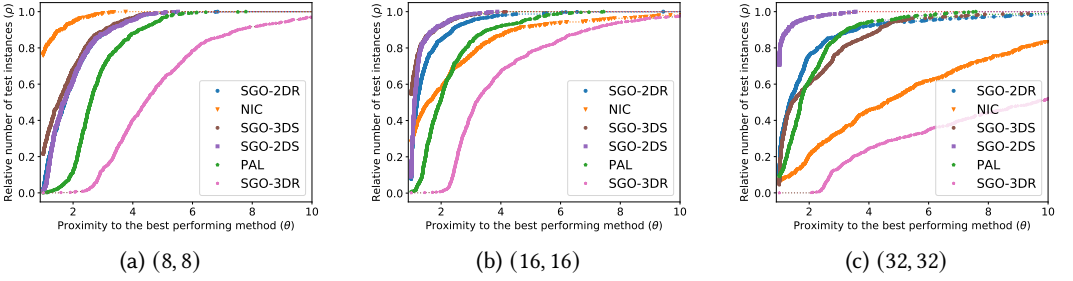


Fig. 8. Performance profile plots of the partitioning methods with natural ordering. The algorithms are compared wrt. their execution times.

PAL and UNI. We observe that the difference between SGO-3DS and other algorithms start to increase as we increase the number of parts from $(8, 8)$ to $(32, 32)$. Among those algorithms only SGO-3DS tries to minimize the objective function (18), we see that minimizing the maximum load of a single partition also helps in most cases as SGO-2DS seems to perform relatively well. The reason for this phenomenon is that 3 times (16) is an upper bound for (18), so optimizing for (16) also implicitly optimizes for (18).

6.3 Evaluation of the Execution Time

We would like to note that in this work our goal is to propose a novel subgradient-based multi-dimensional rectilinear partitioning framework. However, to achieve better performance we enabled parallelization features using modern C++ execution policies and also we transformed pleasingly parallelizable loops in to parallel. All of the algorithms used for the experiments were parallelized in the same manner including the sparse prefix sum data structure. We include data structure construction time and partitioning time in reported execution times. Among the RPP algorithms, we pick NIC as the baseline omitting 4APX and 2SWP as NIC is the only algorithm that gives comparable results to SGO-2DR. The execution time of 2SWP is around 5 to 10 times faster than NIC because it only does 2 iterations whereas NIC can do upto 20 iterations. Even though 4APX does more iterations than SGO-2DR and requires a binary search on top as the algorithm is presented in the format of a decision procedure, it still gives worse results and the runtime of a single iteration is the same as SGO-2DR as they both use the same sparse prefix sum data structure to query loads of tiles in each iteration.

In Figure 8, we observe that when we increase the number of parts the NIC algorithm gives worse performance; as we go from $k = (k_1, k_2) = (8, 8)$ to $(32, 32)$. Because the complexity of the NIC algorithm depends on $k_1 + k_2$ linearly and other algorithms' runtimes are mostly dominated by the sparse prefix sum data structure construction time, which doesn't depend on k . In addition, we observe that different variants of SGORP are at least as fast as the PAL algorithm, while SGO-2DS being around more than 2 times faster on average. Since SGO-3DR partitions two matrices simultaneously and has to build two different sparse prefix sum data structures and query them during each iteration, it does at least 2 times as much work as other algorithms. It also optimizes over 3 partition arrays which increases the dimensionality of the searches space by 3 times. That is why it is much slower than other SGORP variants.

7 CONCLUSION

In this paper, we propose an efficient iterative subgradient-based method, SGORP, for the rectilinear partitioning problem that is generalizable for arbitrary d dimensions. We also show our framework

can solve the symmetric rectilinear partitioning problem, via constraints. We propose algorithms to two variants of this problem. Finally, our experiments on more than 600 matrices show that SGORP outperforms state-of-the-art algorithms in terms of partition quality and execution time.

ACKNOWLEDGMENTS

This material is based upon work supported by the National Science Foundation under Grant Number CCF-1919021. This research was supported in part through research cyberinfrastructure resources and services provided by the Partnership for an Advanced Computing Environment (PACE) at the Georgia Institute of Technology, Atlanta, Georgia, USA.

REFERENCES

- [1] Bengt Aspvall, Magnús M Halldórsson, and Fredrik Manne. 2001. Approximations for the general block distribution of a matrix. *Theoretical Computer Science* 262, 1-2 (2001), 145–160.
- [2] Marsha J Berger and Shahid H Bokhari. 1987. A partitioning strategy for nonuniform problems on multiprocessors. *IEEE Trans. Comput.* 5 (1987), 570–580.
- [3] Francine Berman and Lawrence Snyder. 1987. On Mapping Parallel Algorithms into Parallel Architectures. *J. Parallel Distrib. Comput.* 4, 5 (Oct. 1987), 439–458.
- [4] Stephen Boyd, Lin Xiao, and Almir Mutapcic. 2003. Subgradient methods. *lecture notes of EE392o, Stanford University, Autumn Quarter 2004* (2003), 2004–2005.
- [5] Aydin Buluç and John R Gilbert. 2012. Parallel sparse matrix-matrix multiplication and indexing: Implementation and experiments. *SIAM Journal on Scientific Computing* 34, 4 (2012), C170–C191.
- [6] Ümit V. Çatalyürek and Cevdet Aykanat. 1999. Hypergraph-Partitioning Based Decomposition for Parallel Sparse-Matrix Vector Multiplication. *IEEE Transactions on Parallel and Distributed Systems* 10, 7 (1999), 673–693.
- [7] Peter Sanders David A. Bader, Henning Meyerhenke and Dorothea Wagner. 2012. 10th DIMACS Implementation Challenge - Graph Partitioning and Graph Clustering. <https://www.cc.gatech.edu/dimacs10/downloads.shtml>.
- [8] Timothy A Davis and Yifan Hu. 2011. The University of Florida sparse matrix collection. *ACM Transactions on Mathematical Software (TOMS)* (2011), 1.
- [9] Gunduz Vehbi Demirci and Cevdet Aykanat. 2020. Cartesian Partitioning Models for 2D and 3D Parallel SpGEMM Algorithms. *IEEE Transactions on Parallel and Distributed Systems* 31, 12 (2020), 2763–2775.
- [10] Mehmet Deveci, Christian Trott, and Sivasankaran Rajamanickam. 2018. Multithreaded sparse matrix-matrix multiplication for many-core and GPU architectures. *Parallel Comput.* 78 (2018), 33–46.
- [11] Elizabeth D Dolan and Jorge J Moré. 2002. Benchmarking optimization software with performance profiles. *Mathematical programming* 91, 2 (2002), 201–213.
- [12] Daya Ram Gaur, Toshihide Ibaraki, and Ramesh Krishnamurti. 2002. Constant ratio approximation algorithms for the rectangle stabbing problem and the rectilinear partitioning problem. *Journal of Algorithms* 43, 1 (2002), 138–152.
- [13] Michelangelo Grigni and Fredrik Manne. 1996. On the complexity of the generalized block distribution. In *International Workshop on Parallel Algorithms for Irregularly Structured Problems*. 319–326.
- [14] Song Guo and Xiaolin Hu. 2011. Profile-based spatial partitioning for parallel simulation of large-scale wildfires. *Simulation Modelling Practice and Theory* 19, 10 (2011), 2206–2225.
- [15] Bruce Hendrickson and Tamara G Kolda. 2000. Graph partitioning models for parallel computing. *Parallel computing* 26, 12 (2000), 1519–1534.
- [16] Yang Hu, Hang Liu, and H Howie Huang. 2018. Tricore: Parallel triangle counting on gpus. In *SC18: International Conference for High Performance Computing, Networking, Storage and Analysis*. IEEE, 171–182.
- [17] H Karimabadi, HX Vu, D Krauss-Varban, and Y Omelchenko. 2006. Global hybrid simulations of the Earth’s magnetosphere. In *Numerical Modeling of Space Plasma Flows*, Vol. 359. 257.
- [18] George Karypis and Vipin Kumar. 1998. A fast and high quality multilevel scheme for partitioning irregular graphs. *SIAM Journal on scientific Computing* 20, 1 (1998), 359–392.
- [19] Sanjeev Khanna, Shanmugavelayutham Muthukrishnan, and Steven Skiena. 1997. Efficient array partitioning. In *International Colloquium on Automata, Languages, and Programming*. 616–626.
- [20] Matthieu Latapy. 2008. Main-memory triangle computations for very large (sparse (power-law)) graphs. *Theoretical Computer Science* (2008), 458–473.
- [21] Jeongmyung Lee, Seokwon Kang, Yongseung Yu, Yong-Yeon Jo, Sang-Wook Kim, and Yongjun Park. 2020. Optimization of GPU-based Sparse Matrix Multiplication for Large Sparse Networks. In *2020 IEEE 36th International Conference on Data Engineering (ICDE)*. IEEE, 925–936.

- [22] Paul Lin, Matthew Bettencourt, Stefan Domino, Travis Fisher, Mark Hoemmen, Jonathan Hu, Eric Phipps, Andrey Prokopenko, Sivasankaran Rajamanickam, Christopher Siefert, et al. 2014. Towards extreme-scale simulations for low mach fluids with second-generation trinos. *Parallel processing letters* 24, 04 (2014), 1442005.
- [23] Weifeng Liu and Brian Vinter. 2014. An efficient GPU general sparse matrix-matrix multiplication for irregular data. In *2014 IEEE 28th International Parallel and Distributed Processing Symposium*. IEEE, 370–381.
- [24] Fredrik Manne and Tor Sørveik. 1996. Partitioning an array onto a mesh of processors. In *International Workshop on Applied Parallel Computing*. 467–477.
- [25] Víctor Martínez, Fernando Berzal, and Juan-Carlos Cubero. 2016. A survey of link prediction in complex networks. *ACM computing surveys (CSUR)* 49, 4 (2016), 1–33.
- [26] S. Muthukrishnan and Torsten Suel. 2005. Approximation Algorithms for Array Partitioning Problems. *J. Algorithms* 54, 1 (Jan. 2005), 85–104.
- [27] Saket Navlakha, Rajeev Rastogi, and Nisheeth Shrivastava. 2008. Graph summarization with bounded error. In *Proceedings of the 2008 ACM SIGMOD international conference on Management of data*. 419–432.
- [28] David M. Nicol. 1994. Rectilinear partitioning of irregular data parallel computations. *J. Parallel and Distrib. Comput.* 23, 2 (1994), 119–134.
- [29] John R Pilkington and Scott B Baden. 1996. Dynamic partitioning of non-uniform structured workloads with spacefilling curves. *IEEE Transactions on Parallel and Distributed Systems* 7, 3 (1996), 288–300.
- [30] Steven J Plimpton, David B Seidel, Michael F Pasik, Rebecca S Coats, and Gary R Montry. 2003. A load-balancing algorithm for a parallel electromagnetic particle-in-cell code. *Computer physics communications* 152, 3 (2003), 227–241.
- [31] Erzsébet Ravasz, Anna Lisa Somera, Dale A Mongru, Zoltán N Oltvai, and A-L Barabási. 2002. Hierarchical organization of modularity in metabolic networks. *science* 297, 5586 (2002), 1551–1555.
- [32] Purnamrita Sarkar, Deepayan Chakrabarti, and Andrew W Moore. 2011. Theoretical justification of popular link prediction heuristics.. In *IJCAI proceedings-international joint conference on artificial intelligence*, Vol. 22. Citeseer, 2722.
- [33] Erik Saule, Erdeniz O. Bas, and Ümit V. Çatalyürek. 2012. Load-Balancing Spatially Located Computations using Rectangular Partitions. *J. Parallel and Distrib. Comput.* 72, 10 (2012), 1201–1214.
- [34] N. Z. Shor, Krzysztof C. Kiwiel, and Andrzej Ruszcayundefinedski. 1985. *Minimization Methods for Non-Differentiable Functions*. Springer-Verlag, Berlin, Heidelberg.
- [35] Manuel Ujaldon, Shamik D Sharma, Emilio L Zapata, and Joel Saltz. 1996. Experimental evaluation of efficient sparse matrix distributions. In *International Conference on Supercomputing*. 78–85.
- [36] Robert A Van De Geijn and Jerrell Watts. 1997. SUMMA: Scalable universal matrix multiplication algorithm. *Concurrency: Practice and Experience* 9, 4 (1997), 255–274.
- [37] M. S. Warren and J. K. Salmon. 1993. A Parallel Hashed Oct-Tree N-Body Algorithm. In *Proceedings of the 1993 ACM/IEEE Conference on Supercomputing* (Portland, Oregon, USA) (*Supercomputing '93*). Association for Computing Machinery, New York, NY, USA, 12–21.
- [38] Abdurrahman Yaşar, Muhammed Fatih Balin, Xiaojing An, Kaan Sancak, and Ümit V. Çatalyürek. 2021. On Symmetric Rectilinear Matrix Partitioning. *Journal of Experimental Algorithmics* (2021). <https://doi.org/10.1145/3492220> to appear..
- [39] Abdurrahman Yaşar, Sivasankaran Rajamanickam, Jonathan W. Berry, and Ümit V. Çatalyürek. 2022. A Block-Based Triangle Counting Algorithm on Heterogeneous Environments. *IEEE Transactions on Parallel and Distributed Systems* 33, 2 (Feb 2022), 444–458. <https://doi.org/10.1109/TPDS.2021.3093240>

A APPENDIX

A.1 Detailed results for a small subset of matrices

In order to provide reproducible results, we have provided normalized load imbalance (with respect to average non-zero per part, meaning $\frac{L(f,p)k_1k_2}{L(f)}$) and absolute execution times of the algorithms for a selected subset of the sparse matrices. Table 2 presents the detailed properties of those matrices, total 16 of them. Tables 3 to 8 present the normalized loads and execution times of different algorithms for $k_1 = k_2 \in \{8, 16, 32\}$.

Table 2. The properties of sparse matrices.

| Matrix Name | Matrix Origin | # Rows | # Nonzeros | Density |
|------------------|------------------|-------------|---------------|---------|
| twitter7 | Social | 41,652,231 | 1,468,365,182 | 35.25 |
| uk-2005 | Web | 39,459,926 | 936,364,282 | 23.73 |
| stokes | Semiconductor | 11,449,534 | 349,321,980 | 30.51 |
| kmer_A2a | Biological | 170,728,176 | 180,292,586 | 1.06 |
| nlpkkt160 | Optimization | 8,345,601 | 118,931,856 | 14.25 |
| com-Orkut | Social | 3,072,442 | 117,185,083 | 38.14 |
| kron_g500-logn21 | Kronecker | 2,097,153 | 91,042,010 | 43.41 |
| soc-LiveJournal1 | Social | 4,847,572 | 68,993,773 | 14.23 |
| Cube_Coup_dt6 | Structural | 2,164,761 | 64,685,452 | 29.88 |
| circuit5M | Simulation | 5,558,327 | 59,524,291 | 10.71 |
| hollywood-2009 | Movie/Actor | 1,139,906 | 57,515,616 | 50.46 |
| wb-edu | Web | 9,845,726 | 57,156,537 | 5.81 |
| europe_osm | Road | 50,912,019 | 54,054,660 | 1.06 |
| dielFilterV3real | Electromagnetics | 1,102,825 | 45,204,422 | 40.99 |
| kron_g500-logn20 | Kronecker | 1,048,577 | 44,620,272 | 42.55 |
| road_usa | Road | 23,947,348 | 28,854,312 | 1.20 |

Table 3. The normalized loads of different algorithms for $k_1 = k_2 = 8$ compared wrt. (15).

| | SGO-2DR | NIC | 2SWP | 4APX | SGO-2DS | PAL | UNI |
|------------------|----------------|------------|-------------|-------------|----------------|------------|------------|
| twitter7 | 1.78 | 1.67 | 2.32 | 1.81 | 1.85 | 1.80 | 9.35 |
| uk-2005 | 5.06 | 5.13 | 6.29 | 7.90 | 7.65 | 7.65 | 11.47 |
| stokes | 2.93 | 2.75 | 3.13 | 4.27 | 4.71 | 4.79 | 5.01 |
| kmer_A2a | 1.95 | 1.84 | 2.27 | 2.43 | 2.63 | 3.33 | 2.51 |
| nlpkkt160 | 4.88 | 5.75 | 6.17 | 13.65 | 9.46 | 7.75 | 14.66 |
| com-Orkut | 2.78 | 2.72 | 2.80 | 2.87 | 2.87 | 2.83 | 5.95 |
| kron_g500-logn21 | 1.83 | 1.89 | 2.48 | 2.01 | 2.49 | 3.16 | 2.08 |
| soc-LiveJournal1 | 2.17 | 2.13 | 2.57 | 2.68 | 2.51 | 2.51 | 15.40 |
| Cube_Coup_dt6 | 4.97 | 7.66 | 6.40 | 7.70 | 7.69 | 7.69 | 7.84 |
| circuit5M | 2.64 | 2.79 | 3.22 | 3.64 | 2.67 | 3.19 | 16.94 |
| hollywood-2009 | 4.20 | 4.01 | 4.75 | 6.88 | 5.78 | 5.78 | 11.05 |
| wb-edu | 4.79 | 5.67 | 6.05 | 7.66 | 7.63 | 7.63 | 8.78 |
| europe_osm | 4.93 | 6.79 | 5.66 | 7.39 | 7.39 | 7.39 | 7.70 |
| dielFilterV3real | 3.06 | 3.00 | 4.88 | 4.45 | 4.66 | 4.09 | 5.60 |
| kron_g500-logn20 | 1.85 | 1.89 | 2.58 | 2.00 | 2.61 | 3.16 | 2.08 |
| road_usa | 5.05 | 5.90 | 5.05 | 6.85 | 6.86 | 6.84 | 7.07 |

Table 4. The normalized loads of different algorithms for $k_1 = k_2 = 16$ compared wrt. (15).

| | SGO-2DR | NIC | 2SWP | 4APX | SGO-2DS | PAL | UNI |
|------------------|----------------|------------|-------------|-------------|----------------|------------|------------|
| twitter7 | 2.07 | 2.00 | 2.91 | 2.16 | 2.17 | 2.13 | 15.12 |
| uk-2005 | 9.37 | 9.83 | 13.87 | 17.43 | 15.21 | 15.20 | 27.09 |
| stokes | 5.43 | 5.33 | 6.10 | 8.21 | 8.52 | 9.06 | 9.06 |
| kmer_A2a | 2.48 | 2.46 | 3.11 | 3.25 | 3.33 | 4.03 | 4.43 |
| nlpkkt160 | 9.25 | 7.98 | 13.34 | 27.11 | 18.06 | 15.46 | 28.83 |
| com-Orkut | 3.58 | 3.53 | 4.64 | 3.84 | 3.62 | 3.59 | 14.03 |
| kron_g500-logn21 | 1.98 | 2.26 | 2.85 | 2.01 | 3.36 | 3.54 | 2.17 |
| soc-LiveJournal1 | 3.10 | 2.94 | 3.80 | 4.57 | 3.88 | 3.88 | 27.47 |
| Cube_Coup_dt6 | 9.92 | 14.26 | 13.78 | 15.35 | 14.74 | 14.73 | 15.52 |
| circuit5M | 4.93 | 5.42 | 5.43 | 6.76 | 5.00 | 4.61 | 26.61 |
| hollywood-2009 | 7.55 | 7.28 | 7.99 | 11.59 | 9.98 | 9.66 | 28.95 |
| wb-edu | 9.42 | 10.41 | 10.11 | 16.16 | 15.21 | 15.21 | 18.22 |
| europe_osm | 8.77 | 10.68 | 9.48 | 14.64 | 14.62 | 14.61 | 15.37 |
| dielFilterV3real | 5.82 | 6.12 | 6.90 | 8.37 | 8.89 | 7.43 | 8.59 |
| kron_g500-logn20 | 2.09 | 2.25 | 3.00 | 2.07 | 3.04 | 3.54 | 2.13 |
| road_usa | 8.94 | 8.94 | 11.14 | 12.32 | 12.30 | 11.48 | 13.23 |

Table 5. The normalized loads of different algorithms for $k_1 = k_2 = 32$ compared wrt. (15).

| | SGO-2DR | NIC | 2SWP | 4APX | SGO-2DS | PAL | UNI |
|------------------|----------------|------------|-------------|-------------|----------------|------------|------------|
| twitter7 | 2.42 | 2.47 | 3.35 | 2.88 | 2.64 | 2.63 | 26.60 |
| uk-2005 | 18.03 | 15.84 | 19.72 | 43.52 | 30.35 | 30.29 | 57.25 |
| stokes | 10.55 | 10.09 | 11.71 | 16.46 | 16.45 | 16.94 | 19.10 |
| kmer_A2a | 4.15 | 3.97 | 5.45 | 5.14 | 5.17 | 5.43 | 7.19 |
| nlpkkt160 | 17.94 | 15.96 | 27.06 | 50.97 | 36.66 | 30.54 | 55.67 |
| com-Orkut | 4.57 | 4.38 | 6.95 | 5.26 | 4.79 | 4.80 | 23.69 |
| kron_g500-logn21 | 2.26 | 2.62 | 3.51 | 2.02 | 3.21 | 3.76 | 2.32 |
| soc-LiveJournal1 | 4.80 | 4.42 | 5.72 | 11.41 | 6.28 | 6.28 | 49.99 |
| Cube_Coup_dt6 | 19.85 | 21.82 | 27.85 | 27.14 | 26.93 | 26.92 | 30.65 |
| circuit5M | 9.55 | 8.46 | 10.44 | 18.17 | 8.66 | 8.68 | 49.37 |
| hollywood-2009 | 12.80 | 12.48 | 14.93 | 40.53 | 17.76 | 17.74 | 93.46 |
| wb-edu | 18.62 | 19.23 | 19.97 | 31.67 | 30.31 | 30.30 | 40.53 |
| europe_osm | 18.05 | 17.88 | 23.94 | 29.07 | 28.98 | 28.97 | 30.65 |
| dielFilterV3real | 11.24 | 11.17 | 12.93 | 16.14 | 16.02 | 14.17 | 17.29 |
| kron_g500-logn20 | 2.45 | 2.63 | 3.72 | 2.02 | 3.29 | 3.76 | 2.40 |
| road_usa | 13.22 | 13.50 | 16.31 | 17.56 | 17.17 | 18.22 | 21.67 |

Table 6. The execution time in seconds of different algorithms for $k_1 = k_2 = 8$.

| | SGO-2DR | NIC | 2SWP | 4APX | SGO-2DS | PAL |
|------------------|----------------|------------|-------------|-------------|----------------|------------|
| twitter7 | 127.76 | 37.38 | 739.04 | 129.64 | 127.79 | 117.90 |
| uk-2005 | 25.17 | 15.45 | 112.86 | 40.37 | 25.17 | 29.93 |
| stokes | 9.98 | 3.93 | 35.65 | 15.22 | 10.00 | 11.36 |
| kmer_A2a | 13.03 | 11.06 | 69.84 | 55.48 | 13.06 | 23.72 |
| nlpkkt160 | 3.76 | 1.59 | 11.77 | 11.34 | 3.76 | 4.64 |
| com-Orkut | 6.00 | 2.15 | 19.15 | 11.66 | 6.02 | 6.63 |
| kron_g500-logn21 | 4.74 | 1.55 | 16.43 | 7.72 | 4.74 | 5.05 |
| soc-LiveJournal1 | 3.38 | 1.54 | 12.45 | 9.08 | 3.39 | 4.44 |
| Cube_Coup_dt6 | 1.62 | 0.42 | 5.98 | 5.99 | 1.62 | 1.96 |
| circuit5M | 1.99 | 1.09 | 5.85 | 5.91 | 1.99 | 2.64 |
| hollywood-2009 | 1.81 | 0.80 | 6.00 | 4.98 | 1.82 | 1.99 |
| wb-edu | 1.88 | 1.19 | 8.49 | 7.11 | 1.88 | 2.64 |
| europe_osm | 3.89 | 2.40 | 15.53 | 18.49 | 3.89 | 7.95 |
| dielFilterV3real | 1.27 | 0.44 | 3.93 | 3.92 | 1.27 | 1.43 |
| kron_g500-logn20 | 2.10 | 0.76 | 7.25 | 4.85 | 2.10 | 2.20 |
| road_usa | 1.77 | 1.41 | 9.77 | 10.42 | 1.78 | 3.29 |

Table 7. The execution time in seconds of different algorithms for $k_1 = k_2 = 16$.

| | SGO-2DR | NIC | 2SWP | 4APX | SGO-2DS | PAL |
|------------------|----------------|------------|-------------|-------------|----------------|------------|
| twitter7 | 127.86 | 44.22 | 753.83 | 135.45 | 127.88 | 118.16 |
| uk-2005 | 25.22 | 33.06 | 116.03 | 45.24 | 25.19 | 29.89 |
| stokes | 10.05 | 8.21 | 32.64 | 21.05 | 10.02 | 11.45 |
| kmer_A2a | 13.21 | 33.33 | 79.05 | 56.92 | 13.10 | 24.34 |
| nlpkkt160 | 3.77 | 3.69 | 12.05 | 13.23 | 3.77 | 4.71 |
| com-Orkut | 6.04 | 2.02 | 18.89 | 13.51 | 6.07 | 6.72 |
| kron_g500-logn21 | 4.80 | 2.08 | 16.69 | 9.19 | 4.81 | 5.13 |
| soc-LiveJournal1 | 3.43 | 3.43 | 12.28 | 11.44 | 3.43 | 4.53 |
| Cube_Coup_dt6 | 1.63 | 0.71 | 6.10 | 6.48 | 1.63 | 2.04 |
| circuit5M | 2.02 | 2.00 | 6.06 | 7.26 | 2.02 | 2.67 |
| hollywood-2009 | 1.84 | 1.77 | 6.37 | 8.39 | 1.84 | 2.08 |
| wb-edu | 1.89 | 3.08 | 9.07 | 11.99 | 1.88 | 2.76 |
| europe_osm | 3.90 | 6.95 | 17.70 | 19.99 | 3.90 | 7.94 |
| dielFilterV3real | 1.30 | 0.65 | 4.04 | 6.55 | 1.28 | 1.50 |
| kron_g500-logn20 | 2.17 | 1.26 | 7.11 | 5.63 | 2.15 | 2.28 |
| road_usa | 1.78 | 5.04 | 10.52 | 13.62 | 1.82 | 3.42 |

Table 8. The execution time in seconds of different algorithms for $k_1 = k_2 = 32$.

| | SGO-2DR | NIC | 2SWP | 4APX | SGO-2DS | PAL |
|------------------|----------------|------------|-------------|-------------|----------------|------------|
| twitter7 | 128.47 | 138.33 | 248.65 | 152.22 | 128.34 | 118.50 |
| uk-2005 | 25.53 | 67.08 | 125.55 | 51.70 | 25.30 | 30.31 |
| stokes | 10.41 | 20.48 | 33.74 | 26.21 | 10.15 | 11.72 |
| kmer_A2a | 13.63 | 54.22 | 82.41 | 65.21 | 13.47 | 25.05 |
| nlpkkt160 | 3.80 | 10.03 | 12.64 | 24.14 | 3.79 | 4.93 |
| com-Orkut | 6.35 | 3.96 | 19.13 | 16.63 | 6.27 | 6.94 |
| kron_g500-logn21 | 5.35 | 3.47 | 16.83 | 12.71 | 5.17 | 5.32 |
| soc-LiveJournal1 | 3.78 | 9.20 | 12.65 | 15.24 | 3.59 | 4.76 |
| Cube_Coup_dt6 | 1.64 | 4.20 | 6.37 | 12.73 | 1.64 | 2.24 |
| circuit5M | 2.16 | 3.55 | 7.02 | 9.11 | 2.11 | 2.86 |
| hollywood-2009 | 2.04 | 4.16 | 6.38 | 10.82 | 1.88 | 2.28 |
| wb-edu | 1.97 | 9.62 | 9.66 | 17.50 | 1.91 | 3.01 |
| europe_osm | 3.98 | 35.89 | 20.03 | 26.20 | 3.92 | 8.46 |
| dielFilterV3real | 1.41 | 2.96 | 4.26 | 10.90 | 1.37 | 1.67 |
| kron_g500-logn20 | 2.73 | 1.82 | 7.13 | 7.39 | 2.53 | 2.44 |
| road_usa | 1.86 | 12.40 | 11.45 | 14.81 | 1.95 | 3.59 |